SCIENTIFIC REPORTS

OPEN

Photo-designed terahertz devices

Takanori Okada[1] & Koichiro Tanaka[2]

[1]Pioneering Research Unit for Next Generation, Kyoto University, Kyoto 615-8520, Japan, [2]Institute for Integrated Cell-Material Sciences, Kyoto University, Kyoto 606-8502, Japan.

SUBJECT AREAS:
TERAHERTZ TECHNOLOGY
OPTICAL PHYSICS
OPTICAL MATERIALS AND STRUCTURES
ULTRAFAST PHOTONICS

Received
25 August 2011

Accepted
30 September 2011

Published
18 October 2011

Correspondence and requests for materials should be addressed to T.O. (t.okada@kupru.iae.kyoto-u.ac.jp)

Technologies are being developed to manipulate electromagnetic waves using artificially structured materials such as photonic crystals and metamaterials, with the goal of creating primary optical devices. For example, artificial metallic periodic structures show potential for the construction of devices operating in the terahertz frequency regime. Here we demonstrate the fabrication of photo-designed terahertz devices that enable the real-time, wide-range frequency modulation of terahertz electromagnetic waves. These devices are comprised of a photo-induced, planar periodic-conductive structure formed by the irradiation of a silicon surface using a spatially modulated, femtosecond optical pulsed laser. We also show that the modulation frequency can be tuned by the structural periodicity, but is hardly affected by the excitation power of the optical pump pulse. We expect that our findings will pave the way for the construction of all-optical compact operating devices, such as optical integrated circuits, thereby eliminating the need for materials fabrication processes.

Terahertz radiation (1 THz = 10^{12} Hz), which is commonly defined as the region of the electromagnetic spectrum between 0.3 THz and 10 THz, is extremely attractive for a variety of applications in science and technology such as sensing, imaging, and telecommunication[1]. Because exploration of this spectral region located between radio and optical frequencies is only at the initial stages, many further applications in diverse fields are also expected. One envisaged technology involves the development of high-speed and high-frequency operating devices in the field of ultrafast optical communication, which has the potential to replace conventional electric circuits. In order to realize applications such as optical switching devices, control of the frequency characteristics over a wide frequency range is important.

Previous studies have verified that THz pulses can be guided using metal wires[2,3], and that the frequency modulation can be tuned by artificial periodic metal structures[4,5] when the geometry and dimensions are appropriately scaled[6,7]. Furthermore, the real-time optical control of THz pulses has been achieved by the application of a bias voltage in so-called active terahertz metamaterials[8], by the injection of photo-induced charge carriers into metamaterial arrays[9,10], and by the use of reconfigurable metamaterials that respond to external stimuli[11]. The dynamic control of metamaterials has great potential for use in applications such as optical modulators with temporally and geometrically varying patterns, as well as in the active control of optical filters[12,13]. However, the modulation frequency has thus far been limited to a small region around the resonance frequency determined by the fixed structural geometry, allowing only narrow frequency shifts. In order to overcome this limitation, we propose and demonstrate the operation of a photo-designed THz device in which the period, shape and dimension of the photo-induced planar structural pattern can be varied dynamically.

Results

The planar photo-induced structures used in this study were one-dimensional periodical rectangular corrugations (namely, line grating (LG) patterns), which were created by focusing a spatially phase-modulated femtosecond laser pulse on a high-resistivity Si ($R > 1000$ Ω•cm) surface. The fabrication system and the geometry of the LG structure are shown in Fig. 1a. The optical pump pulse wavelength of 800 nm allows the excitation of carriers to the conduction band, the spatial distribution of which on the silicon (Si) surface can be controlled using a liquid-crystal spatial light modulator (SLM), as shown in Fig. 1b (see Methods). This enables the creation of arbitrary beam patterns with periodicities that can be varied freely. The lines comprising the LG pattern were well defined, as shown in the optical microscope image in Fig. 1c, although small spatial fluctuations of the photo-induced carrier density might be inherent[14]. The period of the LG structure was varied from a = 100 μm to 300 μm; the width of each line in Fig. 1c corresponds to one-half of this period. The optical pump power (P_{pump}) was varied from 4 mW to 100 mW, which gave a corresponding carrier density at the Si surface (N_{pump}) of between 1.1×10^{16} cm^{-3} and 2.7×10^{17} cm^{-3}, and a plasma frequency (f_p) of between 0.7 THz and 3.4 THz. These values were calculated using the relationship $f_p = (N_{pump}e^2/\varepsilon_0\varepsilon_{Si}\mu)^{1/2}$, where $1/\mu = 1/m_e + 1/m_h$ is a

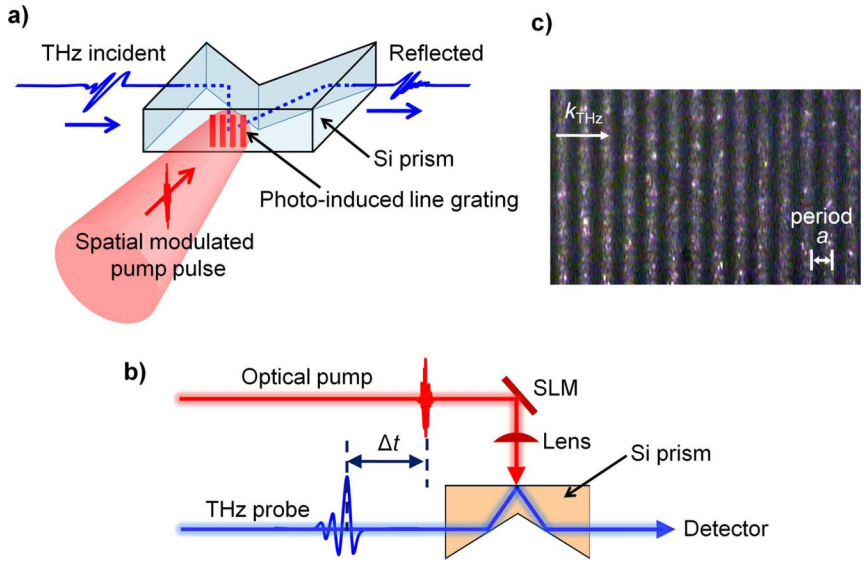

Figure 1 | Fabrication and experimental operation of photo-designed THz devices. (a) Fabrication of a planar photo-induced LG pattern at the total reflection surface of a Si prism with refractive index 3.4 in the THz frequency regime. (b) Measurement of surface electromagnetic mode on photo-designed THz devices (see Methods). (c) Optical microscope image of photo-induced LG pattern taken with an infrared sensor viewer for better contrast. Fluctuations in brightness within the lines are due to scattered light at the rough surface of the viewer. The periodicity of the pattern is parallel to the THz wave vector $\boldsymbol{k}_{THz}$.

function of the reduced masses of the electron and the hole, $m_e = 0.27m_0$ and $m_h = 0.37m_0$ are the effective masses of electrons and holes in Si[15], ε_0 is the permittivity of free space, $\varepsilon_{Si} = 11.6$ is the permittivity of Si in the THz frequency regime, e is the electron charge, and m_0 is the electron rest mass.

We employed an internal-reflection configuration for our measurement (see Methods), checking that no undesired THz emission from optical excitation inside the Si occurred[16]. The optical-pump and THz-probe technique was used to characterize the performance of the photo-designed THz devices, as shown in Fig. 1b. We note that diffraction between the pump and probe pulses, as observed for holograms and population gratings[14,17–19], should be prevented here because the frequency of the optical pulses was much higher than that of the probe pulses. The timing of the optical excitation was $\Delta t = 50$ ps before the arrival of the THz probe pulse at the Si surface; this time delay was large compared with the rise time of the photocarriers, and sufficiently shorter than the photocarrier lifetime in bulk Si crystals[20,21]. Furthermore, diffusion effects were expected to be negligible, because the diffusion length of the photocarriers is 0.5 μm at 50 ps after excitation[19]. Therefore, the quasi-steady-state properties of the photo-designed THz devices could be investigated as a function of the carrier density, which was determined by the excitation power. Reflectance spectra were obtained using THz time-domain spectroscopy, which is described elsewhere[1,22].

The frequency-dependent reflected intensity is plotted as a function of the LG period in Fig. 2. Here, P_{pump} was set to a constant value of 40 mW, for which the corresponding carrier density at the Si surface is $N_{pump} \approx 1.1 \times 10^{17}$ cm^{-3} and the corresponding plasma frequency is $f_p \approx 2.1$ THz. No characteristic features, except for a broad minimum around 2 THz, were observed in reflection spectrum of a reference photo-induced film (in which the whole area occupied by the LG pattern was uniformly irradiated at the same carrier density of $N_{pump} \approx 1.1 \times 10^{17}$ cm^{-3}). By contrast, a sharp minimum at lower frequencies was observed for all the LG structures; no broad minimum was evident. No significant changes in the spectra were observed upon varying Δt between 5 ps and 300 ps. This was consistent with previously reported ambipolar-diffusivity measurements made using the population-grating method, from which a carrier diffusion length of 1.3 μm was estimated at 300 ps (ref. 19).

As shown in Fig. 2, the frequency of the characteristic sharp minimum could be widely modulated from 0.4 THz to 1.2 THz by deliberately decreasing the period of the LG pattern.

The dependence of the modulated frequency on the periodicity is shown in Fig. 3. The frequency of the sharp minimum increased as the periodicity decreased, in good agreement with theoretical considerations, where the surface electromagnetic mode is assumed to be on the periodic structure[23–26]. The theoretical curve in Fig. 3 was obtained using the approximation from the modal expansion method[25], where $f_{SW} \approx c/[a(\varepsilon_{Si}^{1/2}\sin\theta + 1)]$, under the reasonable assumption of a thin, conductive and planar LG structure; c is the velocity of light in vacuum and θ is the incident angle of 30°. Our

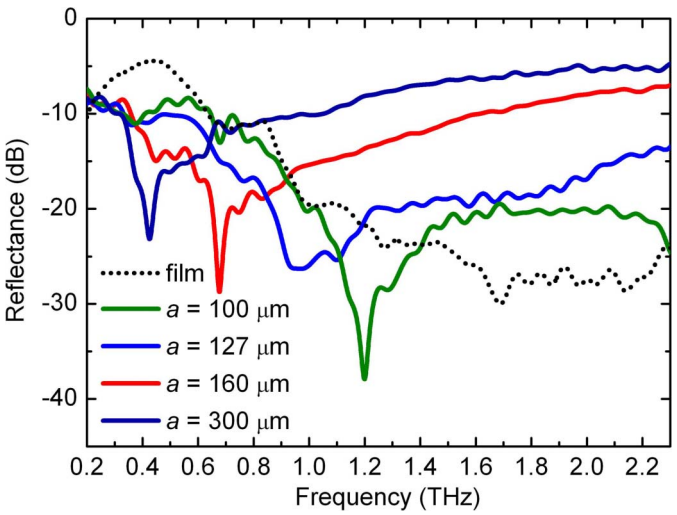

Figure 2 | Modulation performance of photo-designed THz devices as a function of the period of the photo-induced LG. The solid lines represent a series of reflectance spectra from photo-induced LG structures with various periods. The dotted line represents the spectrum for the reference photo-induced film at the same carrier density. The reflection spectrum with no optical pump pulse irradiation is employed in order to normalize the data.

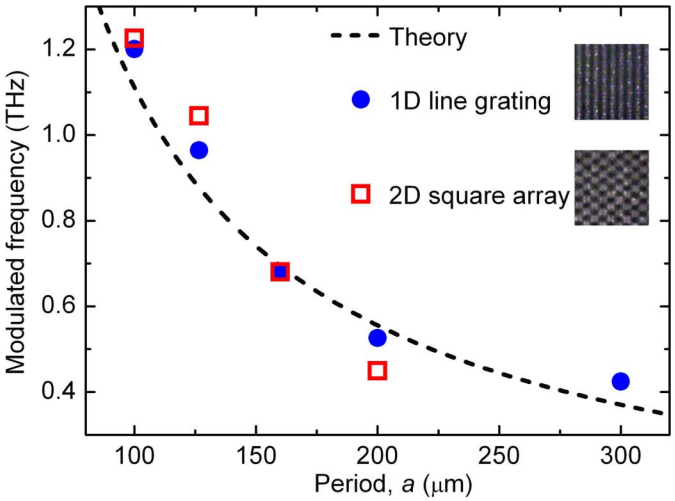

Figure 3 | Dependence of spectral minimum frequency on structural periodicity in photo-designed THz devices. Schematic representations of the one-dimensional LG (blue circular data points) and the two-dimensional square array patterns (red square data points) are shown in the inset. White and black areas indicate irradiated and non-irradiated parts, respectively; the wave vector of the THz pulses $\boldsymbol{k}_{\mathrm{THz}}$ is in the horizontal direction. The theoretical curve obtained under the assumption of the surface electromagnetic mode is shown as a dashed line.

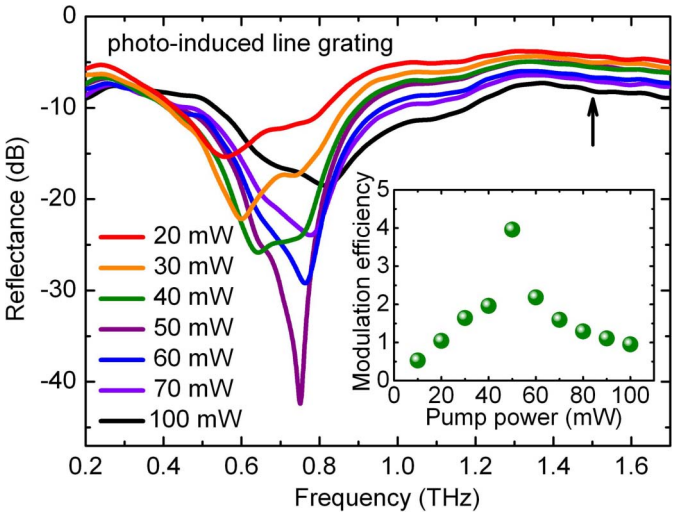

Figure 4 | Modulation performance of a photo-designed THz device as a function of optical pump power. The period of the LG structure measured was fixed at $a = 170$ μm. A minimum frequency of 0.65 THz was calculated under the assumption of the surface electromagnetic mode. The reflection spectrum with no optical pump pulse irradiation is employed in order to normalize the data. The inset shows the modulation efficiency of the reflectance at the minimum as a function of optical pump power. The reference reflectance was set at a frequency of 1.5 THz, indicated by the black arrow.

results thus imply that the photo-induced structure is similar to a planar conductive structure. We also investigated the dependence of the spectral minimum on the periodicity of a two-dimensional square array (each square in the illustration shown in the inset of Fig. 3 occupies half a period). The corresponding reflectance spectra are shown in Supplementary Fig. S1. The same trend of the characteristic spectral minimum with respect to periodicity was observed for the square array, suggesting that the frequency of the minimum is primarily dependent on the periodicity of the structure and not on the pattern, because the structure is much thinner than the THz wavelength due to the skin depth of Si (12.2 μm) at a wavelength of 800 nm[27].

Because the photo-induced carriers forming the LG structure occupy a smaller surface area interacting with the THz probe pulses than the reference photo-induced film, one would expect that the attenuation due to conductivity losses is lower than in the reference film[2]. Therefore, a sharp signal from the surface electromagnetic mode should become clearly observable. Nevertheless, the conductivity losses are still inherently associated with the photo-induced structure[13] over the entire THz probe frequency range. It is informative to consider the dependence of reflectance on the photon-induced carrier density.

Figure 4 shows the transient evolution of the reflectance spectra at different values of pump photon power (P_{pump}) in the case of a photo-induced LG with $a = 170$ μm (the calculated frequency of the minimum is 0.65 THz). As the excitation pump power increased, the reflectance dip (the spectral minimum in the region of 0.7 THz) initially became deeper and sharper, with an accompanying decrease in reflectance over the entire frequency range. The spectral minimum was blue shifted from 0.54 THz to 0.83 THz as P_{pump} increased, and the minimum value of reflectance was found at $P_{\mathrm{pump}} \approx 50$ mW ($N_{\mathrm{pump}} \approx 1.3 \times 10^{17}$ cm^{-3} and $f_{\mathrm{p}} \approx 2.4$ THz). With further increase in P_{pump}, the reflectance dip decreased and eventually became inconsequential. We note that the spectral minimum appears only at $P_{\mathrm{pump}} > 10$ mW, a value corresponding to $f_{\mathrm{p}} \approx 1.1$ THz, which is larger than the frequency of the spectral minimum ($f_{\mathrm{p}} > f_{\mathrm{SW}}$). This implies that the spectral minimum does not arise from modulation of the refractive index as occurs in photonic crystals and electromagnetically induced gratings[17–19].

Discussion

In order to interpret these observations quantitatively, we evaluated the modulation efficiency of the reflectance given by $-\log_{10}|R_{\mathrm{ex}}(f_{\mathrm{min}})/R_{\mathrm{ex}}(f_{\mathrm{ref}})|^2$, where $R_{\mathrm{ex}}(f)$ is the reflectance, f_{min} is the frequency at the spectral minimum, and f_{ref} is the reference frequency; here, we used 1.5 THz (far enough from the minimum) as a typical f_{ref}. The modulation efficiency reaches a maximum at $P_{\mathrm{pump}} \approx 50$ mW, as shown in the inset of Fig. 4, corresponding to the power at which the sharpest minimum was observed. The frequency here is slightly higher than the calculated value of 0.65 THz. This discrepancy cannot be due to the finite thickness of the structure because the frequency of the minimum should be constant with respect to thickness[28]. In the internal reflection configuration used in our study, residual carriers excited by the previous pump pulse (1 ms before the current measurement) may disturb the reflectance spectrum under high-power excitation (Supplementary Figure S2). The blue shift of the minimum would then be caused by a reduction of the effective permittivity of Si due to the existence of diffused residual carriers. Because the density of diffused residual carriers depends on the photo-irradiated surface area, the excitation intensity should be optimized for each particular photo-induced structure in order to achieve high modulation efficiencies for practical applications. We note that the frequency of the minimum can be significantly modulated by the period of the structure, but the excitation pump power has a much smaller influence. This suggests that the sharp minimum cannot be attributed to the waveguide mode that characteristically shifts on varying the thickness of the structures[28].

For the realization of higher performance photo-designed THz switching devices, the quality factor of the surface electromagnetic mode (the width of the minimum) should be improved. One conceivable approach is to reduce the surface area of the photo-irradiated lines without changing the period. In addition, further optimization of the spatial distribution of the photo-induced carrier density in the photo-irradiated part of the structure should also be effective, for example, by the utilization of computer-generated holograms calculated using an iterative Fourier transform algorithm[14]. It is important to note that photo-designed THz devices would also be

usable in a transmission configuration with normal THz incidence. In this configuration, modifications to control the thickness of the structure that interacts with the THz probe pulses would be necessary in order to increase the modulation efficiency, for example, two-photon excitation. This solution would be applicable to our experimental configuration because the densities of the photo-induced carriers and the corresponding plasma frequencies exponentially decrease with depth inside the Si prism in the direction perpendicular to the surface[22]. Moreover, the maximum modulation speed in switching devices is limited by the lifetime of the photo-induced carriers in the Si or the response time of the SLM. The bulk recombination lifetime of the carriers is of the order of 10 μs[20,21] at a low optical pump power, which could improve the operating speed of devices such as present-day electrical switching devices[7,29]. However, ultrashort lasers such as femtosecond pulse lasers are preferable and indispensable for practical use in photo-designed THz devices. Rapid and stable modulation performance using time and space variations of the photo-induced structures can be realized by brief optical excitation in order to prevent distribution changes of the photo-carrier[19,22] during the modulation, while still generating sufficient photocarrier density. The switching speed could be improved by choosing a suitable semiconductor, for example a direct semiconductor such as GaAs, or by using a thin Si film[30], which would also reduce the conductivity losses. In the case of semiconductors with shorter bulk recombination lifetimes such as low-temperature-grown GaAs, it is also necessary to consider the limitation that arises from the greater surface recombination velocity, which causes a much faster decrease of the surface carrier density. The use of a ferroelectric liquid-crystal SLM might also allow the switching speed to be improved. Furthermore, a semiconductor with a small self-diffusion coefficient would be an appropriate choice. This solution could enable the utilization of an electrically modulated continuous-wave laser diode as the optical pump source in photo-designed THz devices.

This work represents the first step towards realizing a novel technology for the wide-range frequency modulation of the THz regime, as well as towards establishing techniques for the real-time operation of the photo-induced structures that make frequency modulation possible. That is, we have established a route towards the real-time creation, modulation, and removal of arbitrary photo-induced structures while eliminating the need for fabrication processes or electrical connections. The experimental demonstration of our technique has other significant implications, such as the ability to control optical responses by dynamical breaking of the symmetry properties of the crystals. This work also has potential to open new technology to realize hybrid switching devices that utilize both conventional surface plasmons with flat surfaces and mimicking (or designer) surface plasmons[24,26] with structured surfaces.

Methods

The surface electromagnetic mode of our photo-designed THz devices was investigated using the internal-reflection configuration (Fig. 1b) with *p*-polarized THz probe pulses (incidence angle 30°). This setup uses a non-coaxial configuration between the pump and probe pulses, which is convenient for both practical use and better modulation efficiency. Propagation of the surface electromagnetic mode gives rise to a large modulation of the THz reflection signals. The modulation efficiency can be quantitatively investigated as a function of frequency, because the intensity of the THz incident wave can easily be obtained by cutting the optical pump pulse (the attenuated total reflection configuration), which is not possible using the normal reflection configuration. The beam waist of the THz pulses at the Si surface was 3.8 mm (smaller than the photo-irradiated area), and the Rayleigh range was 76.4 mm, which indicates that the THz pulse can be regarded as a plane wave (these values were calculated for a frequency of 1 THz). The THz probe wave vector $\boldsymbol{k}_{\mathrm{THz}}$ (transverse magnetic or TM mode) was perpendicular to the LG structure (Fig. 1c). The optical pump pulses were generated by a Ti:sapphire regenerative amplifier (Spitfire, Spectra Physics Inc.) with a centre of wavelength of 800 nm, a power of 800 μJ/pulse, a repetition rate of 1 KHz and a pulse duration of 130 fs. The same system was used to generate the *p*-polarized THz probe pulses. The beam pattern focused at the Si surface to create both the photo-induced LG and square array structures was modulated using a phase-only liquid-crystal SLM (PLUTO, HOLOEYE Inc.). The computer-generated holograms of the LG (or square array) patterns were obtained using an inverse 2D Fourier transform algorithm, addressed to the SLM, and then stored on it. The phase of the laser pulse from a regenerative amplifier is spatially modulated by the reflection at the SLM. The SLM is separated from the lens shown in Fig. 1b, a so-called Fourier lens, by the focal length of the lens. The 2D Fourier transform of the phase-modulated pulse from the SLM is performed by the Fourier lens, yielding the LG (or square array) intensity patterns on the Si surface. A reference film, in which the whole area occupied by the LG pattern was uniformly irradiated, was also examined. In this case, the SLM was replaced by a mirror, and the lens shown in Fig. 1b was removed.

1. Tonouchi, M. Cutting-edge terahertz technology. *Nature Photon.* **1**, 97–105 (2007).
2. Wang, K. & Mittleman, D. M. Metal wires for terahertz wave guiding. *Nature* **432**, 376–379 (2004).
3. Sommerfeld, A. *Electrodynamics* (Academic Press, New York, 1952).
4. Yablonovitch, E. Inhibited spontaneous emission in solid-state physics and electronics. *Phys. Rev. Lett.* **58**, 2059–2062 (1987).
5. Veselago, V. G. The electrodynamics of substances with simultaneously negative values of ε and μ. *Sov. Phys. Usp.* **10**, 509–514 (1968).
6. Yen, T. J. *et al.* Terahertz magnetic response from artificial materials. *Science* **303**, 1494–1496 (2004).
7. Chen, H. T., O'Hara, J. F., Azad, A. K. & Taylor, A. J. Manipulation of terahertz radiation using metamaterials. *Laser Photonics Rev.* **5**, 513–533 (2011).
8. Chen, H. T. *et al.* Active terahertz metamaterial devices. *Nature* **444**, 597–600 (2006).
9. Padilla, W. J., Taylor, A. J., Highstrete, C., Lee, M. & Averitt, R. D. Dynamical electric and magnetic metamaterial response at terahertz frequencies. *Phys. Rev. Lett.* **96**, 107401 (2006).
10. Chen, H. T. *et al.* Experimental demonstration of frequency-agile terahertz metamaterials. *Nature Photon.* **2**, 295–298 (2008).
11. Tao, H. *et al.* Reconfigurable terahertz metamaterials. *Phys. Rev. Lett.* **103**, 147401 (2009).
12. Janke, C., Gómez-Rivas, J., Haring Bolivar, P. & Kurz, H. All-optical switching of the transmission of electromagnetic radiation through subwavelength apertures. *Opt. Lett.* **30**, 2357–2359 (2005).
13. Hendry, E. *et al.* Optical control over surface-plasmon-polariton-assisted THz transmission through a slit aperture. *Phys. Rev. Lett.* **100**, 123901 (2008).
14. Hayasaki, Y., Sugimoto, T., Takita, A. & Nishida, N. Variable holographic femtosecond laser processing by use of a spatial light modulator. *Appl. Phys. Lett.* **87**, 031101 (2005).
15. Riffe, D. M. Temperature dependence of silicon carrier effective masses with application to femtosecond reflectivity measurements. *J. Opt. Soc. Am. B*, **19**, 1092-1100 (2002).
16. Zhang, X.-C., Hu, B. B., Darrow, J. T. & Auston, D. H. Generation of femtosecond electromagnetic pulses from semiconductor surfaces. *Appl. Phys. Lett.* **56**, 1011–1013 (1990).
17. Eichler, H. J. *et al.* Laser-induced free-carrier and temperature gratings in silicon. *Phys. Rev. B* **36**, 3247–3253 (1987).
18. Sjodin, T., Petek, H. & Dai, H. Ultrafast carrier dynamics in silicon: A two-color transient reflection grating study on a (111) surface. *Phys. Rev. Lett.* **81**, 5664–5667 (1998).
19. Sjodin, T., Li, C.-M., Petek, H. & Dai, H.-L. Ultrafast transient grating scattering studies of carrier dynamics at a silicon surface. *Chem. Phys.* **251**, 205–213 (2000).
20. Dimitropoulos, D., Jhaveri, R., Claps, R., Woo, J. C. S. & Jalali, B. Lifetime of photogenerated carriers in silicon-on-insulator rib waveguides. *Appl. Phys. Lett.* **86**, 071115 (2005).
21. Yablonovitch, E., Allara, D. L., Chang, C. C., Gmitter, T. & Bright, T. B. Unusually low surface-recombination velocity on silicon and germanium surfaces. *Phys. Rev. Lett.* **57**, 249–252 (1986).
22. Beard, M. C., Turner, G. M. & Schmuttenmaer, C. A. Transient photoconductivity in GaAs as measured by time-resolved terahertz spectroscopy. *Phys. Rev. B* **62**, 15764–15777 (2000).
23. Pendry, J. B., Holden, A. J., Stewart, W. J. & Youngs, I. Extremely low frequency plasmons in metallic mesostructures. *Phys. Rev. Lett.* **76**, 4773–4776 (1996).
24. Pendry, J. B., Martín-Moreno, L. & García-Vidal, F. J. Mimicking surface plasmons with structured surfaces. *Science* **305**, 847–848 (2004).
25. García-Vidal, F. J., Martín-Moreno, L. & Pendry, J. B. Surfaces with holes in them: new plasmonic metamaterials. *J. Opt. A: Pure Appl. Opt.* **7**, S97–S101 (2005).
26. Hibbins, A. P., Evans, B. R. & Sambles, J. R. Experimental verification of designer surface plasmons. *Science* **308**, 670–672 (2005).
27. Palik, E. D. (ed.) *Handbook of Optical Constants of Solids III* (Academic Press, San Diego, 1998).
28. López-Rios, T., Mendoza, D., García-Vidal, F. J., Sánchez-Dehesa, J. & Pannetier, B. Surface shape resonances in lamellar metallic gratings. *Phys. Rev. Lett.* **81**, 665–668 (1998).
29. Chan, W. L. *et al.* A spatial light modulator for terahertz beams. *Appl. Phys. Lett.* **94**, 213511 (2009).
30. Lui, K. P. H. & Hegmann, F. A. Ultrafast carrier relaxation in radiation-damaged silicon on sapphire studied by optical-pump–terahertz-probe experiments. *Appl. Phys. Lett.* **78**, 3478-3480 (2001).

Acknowledgements
We thank K. Tanaka and M. Nagai for fruitful discussions, and K. Hirao for assistance with the measurement system. This study was supported by the Program for Improvement of Research Environment for Young Researchers from the Special Coordination Funds for Promoting Science and Technology (SCF) commissioned by the Ministry of Education, Culture, Sports, Science and Technology (MEXT) of Japan, by a Grant-in-Aid from the Murata Science Foundation, and by the Research Foundation for Opto-Science and Technology.

Author Contributions
T.O. planned and organized the project, conducted the measurements, calculations and analysis, and wrote the manuscript with additional input from K.T.

Additional information
Supplementary Information accompanies this paper at http://www.nature.com/scientificreports

Competing financial interests The authors declare no competing financial interests.

License: This work is licensed under a Creative Commons Attribution-NonCommercial-ShareAlike 3.0 Unported License. To view a copy of this license, visit http://creativecommons.org/licenses/by-nc-sa/3.0/

How to cite this article: Okada, T. & Tanaka, K. Photo-designed terahertz devices. *Sci. Rep.* **1**, 121; DOI:10.1038/srep00121 (2011).